Send Orders of Reprints at reprints@benthamscience.net

The Natural Products Journal, **2013**, *3*, 15-25

Deciphering the Inactivation of Human Pancreatic α-Amylase, an Anti-diabetic Target, by Bisdemethoxycurcumin, a Small Molecule Inhibitor, Isolated from *Curcuma longa*

Sudha Ponnusamy[a], Smita Zinjarde[a], Shobha Bhargava[b], Urmila Kulkarni-Kale[c], Sangeeta Sawant[c], and Ameeta Ravikumar[a,*]

[a]*Institute of Bioinformatics and Biotechnology, University of Pune 411007, India;* [b]*Molecular Embryology Laboratory, Department of Zoology, University of Pune 411007, India;* [c]*Bioinformatics Centre University of Pune 411 007, India*

Abstract: Natural products from plants are an excellent source of Human pancreatic α-amylase (HPA) inhibitors which have therapeutic application as oral agents to control blood glucose levels. The mechanism of action by Bisdemethoxycurcumin (BDMC) has been reported, isolated from *Curcuma longa* rhizomes, which inactivates HPA, a target for type-2 diabetes. This study validates its mode of action and its target which has to date remained largely unknown. The cytotoxicity and bioactivity of crude extract and BDMC on the pancreatic acinar AR42J secretory model cell line were evaluated with LD_{50} value of 16.25 µg ml^{-1} and 63.53 µM, and secretory α-amylase inhibition of 41% and 30%, respectively. BDMC uncompetitively inhibits HPA (K_i' of 10.1µM) and a binding affinity (K_a) of 8.5 x 10^4 M^{-1} with the involvement of surface exposed aromatic residues. The thermodynamic parameters suggest that binding is both enthalpically and entropically driven with ΔG^o of - 28.13 kJ mol^{-1}. Computational ligand docking showed that inactivation depends on hydrogen bonding and π-π interactions. Thus, BDMC, a natural product could be lowering post-prandial glycemia *via* a novel mode of binding and inactivation of HPA and may proved to be a good drug candidate to reduce/control post-prandial hyperglycemia.

Keywords: Human pancreatic α-amylase, bisdemethoxycurcumin, ligand binding, AR42J cell line, docking.

INTRODUCTION

Diabetes mellitus is a carbohydrate metabolic disorder affecting 346 million people worldwide, with the most prevalent form being Non-insulin dependent Diabetes mellitus (NIDDM) associated with post prandial hyperglycemia [1]. Current oral hypoglycemic agents i.e., acarbose, voglibose, miglitol have side effects and the demand for safer biomedicine from Natural products (NP) with lesser side effects is on the rise. Pancreatic α-amylase or α-1,4-glucan-4-glucanohydrolase (E.C. 3.2.1.1), is a key enzyme in the digestive system and catalyses the initial step in hydrolysis of starch to maltose which is eventually degraded to glucose. Hence retardation of starch digestion by the inhibition of enzymes such as α-amylase plays a key role in the control of diabetes [2, 3]. NPs from plants are known to have a wide variety of pancreatic α-amylase inhibitors which are of therapeutic importance as oral hypoglycemic agents in diabetes mellitus with lesser side effects [4]. The chemical diversity of these components present in NPs has tremendous potential for the discovery of molecules with pharmacological activity. The challenge lies in identifying the biological targets for chemical inhibitors and validating their mode of action [5]. The NP extracts are likely to possess numerous primary and secondary metabolites, many of which have not been previously characterized and offer a good alternative for obtaining lead compounds which can lower post-prandial hyperglycemia with lesser side effects. Currently, very few NPs exhibiting anti-diabetic properties are in different stages of clinical trials. Acarbose, voglibose and miglitol derived from microbial sources are currently in use. Dapagliflozin, an analog of phlorizin, a polyphenolic glucoside from root bark of apple tree, is undergoing phase II while trodusquemine, a sulfated amino sterol from dog-fish shark is in phase I clinical trials for type 2 diabetes [6]. Recently, potent inhibitors for human, rat, hog pancreas and intestinal α-amylase and α-glucosidase have been reported from the crude plant extracts but however very few of them have been isolated, characterized and validated with respect to their structure or their target [4, 7, 8].

In our previous study of the 28 plants screened for pancreatic α-amylase inhibitors, the IPE extract of *C. longa* rhizomes exhibited a strong inhibitory effect on HPA [7, 8]. *C. longa*, rhizomes are used in the traditional Indian Ayurvedic medicine for its anti-diabetic, anti-oxidative and anti-inflammatory properties. The efficacy of turmeric to reduce blood glucose levels in experimentally induced diabetic rats has also been reported [9, 10]. Preliminary phytochemical and GC-MS analysis of this crude *C. longa* IPE suggested the presence of curcuminoids, sesquiterpenes

*Address correspondence to this author at the Institute of Bioinformatics and Biotechnology, University of Pune, Pune- 411007, Maharashtra, India; Tel: +91202569133; Fax: 912025690087; E-mail: ameeta@unipune.ac.in

and other phenolics [7]. However, current understanding regarding the bioactive principle responsible for hypoglycemia as well as the mechanism of action is rudimentary and is limited to the anti-oxidant, anti-cancer and anti-inflammatory effects of curcuminoids. The safety of *C. longa* has been studied in various animal models and it is clear that turmeric is non-toxic even at high doses in laboratory animals [11].

In this study, the isolated curcuminoid responsible for the inhibitory action along with the crude extract were evaluated for its bioactivity and cytotoxicity on AR42J (rat pancreatic acinar) cell line, which produces pancreatic α-amylase on induction with glucocorticoids [12]. Enzyme inhibitor kinetics, ligand binding thermodyanamics, *in silico* docking studies were carried out to reveal the mode of lead inhibitor action on HPA.

MATERIALS AND METHODS

HPA and maltopentaose were purchased from Sigma Aldrich, USA. AR42J rat pancreatic cell line was from ATCC-CRL142. Ham's F-12K with L-glutamine culture media, fetal bovine serum, antibiotics streptomycin, penicillin, 3, 5-Dinitrosalicylic acid (DNSA) and (3-(4,5-Dimethylthiazol-2-yl)-2,5-diphenyltetrazolium bromide (MTT) were procured from Himedia Laboratories, Mumbai, India. All other chemicals from local manufacturer were of Analytical grade.

Bioactivity Guided Isolation

In order to isolate the principle bioactive component from the IPE of *C. longa* rhizome, a series of bioassay-guided purification steps was performed as per the protocol mentioned by Revathy *et al.*, 2011 [13] using silica chromatography and HPLC. The identification of the compound exhibiting bioactivity in dexamethasone induces AR42J celline was confirmed by the complete ^{1}H and ^{13}C Nuclear Magnetic resonance (NMR) spectra in dimethyl sulfoxide (DMSO)-d_6 and was identified as BDMC based on the assignments of the chemical shifts (ppm): ^{1}H NMR (DMSO): δ H-1 7.64, H-2 6.8, H-4 6.13, H-6 6.8, H-7 7.64, H-9 7.66, H-10 6.91, H-12 6.91, H-13 7.66 and ^{13}C NMR (DMSO): δ C-1 140.8, C-2 121.2, C-3 183.6, C-4 101.4, C-5 183.6, C-6 121.2, C-7 140.8 C-8,8' 126.2, C-9,9' 130.8, C-10,10' 116.3, C-11 11' 160.2, C-12,12' 116.3, C-13,13' 130.8. This was found to be in agreement with the spectral analysis and chemical shift data reported in literature [14].

Culturing of AR42-J Cell Line

AR42J cells were cultured in Ham's F-12K with L-glutamine culture media supplemented with nonessential amino acids, sodium pyruvate, 7.5 % sodium bicarbonate, 20% fetal bovine serum and antibiotics (100 µg/ml streptomycin, 100 units/ml penicillin) at 37°C under a humidified condition of 95 % air and 5 % CO_2.

Cytotoxicity and Bioactivity in AR42J Cell Line

Cells were routinely plated at 1×10^5 cells/ml/well onto 12 wells culture dish. After overnight attachment of the cells, the culture medium was replaced by fresh medium with extract and individual curcuminoids predisolved in serum at a concentration of 5-30 μgml^{-1} and 10-100 μMml^{-1} for 24 h. The amount of α-amylase released by cells was determined in an aliquot of medium by DNSA method with starch as the substrate with appropriate controls [7]. At the end of the 24-h incubation period and aspiration of culture media needed from all samples for determination of amylase activity, 20 µl of MTT tetrazolium bromide 5 mg ml^{-1} was added to each sample well containing 500 µl of fresh culture media and AR42J. Cells were incubated for 3 h in the presence of MTT tetrazolium bromide at 37°C. Metabolically active cells reduce MTT to insoluble purple formazan dye crystals, which were dissolved by addition of 500 µl DMSO solution at the end of the incubation period. Obtaining absorption readings at 550 nm using the microplate spectrophotometer (Molecular device, M5, Germany) performed quantitation of solubilized formazan [15].

To determine the efficiency of the inhibitors in the presence of starch, the substrate for α-amylase, at the concentration of both crude and BDMC exhibiting maximum secretary pancreatic α-amylase inhibition, starch load varying from 0.25-1% (w/v) were subjected to dexamethasone induced AR42J cell line.

Mechanism of Inhibition

To reveal the mechanism of BDMC inhibition, kinetics, ligand binding, thermodynamics of binding *in silico* docking studies with HPA were performed.

Kinetics of Enzyme Inhibition

The mode of inhibition of HPA by BDMC was determined by using Michaelis-Menton and Lineweaver-Burk (LB) equations. Maltopentaose (0.05-0.4 mM) was incubated with BDMC-HPA for 2.5 min and the residual enzyme activity was determined by Somogyi's method [16]. Secondary Bowden plots of [S]/V vs [I] were used to determine the dissociation constants (K_i') of lead inhibitor [17].

Rate Constant of Reaction

Rate constants of the reaction were determined by the incubation of HPA (0.2-0.5 U) with differing concentrations of BDMC (0.022-0.032 mM) for varying time points (2.5-15 min) and assayed with starch by DNSA method [7].

One unit of enzyme activity is defined as the amount of enzyme required to release one micromole of maltose from starch/maltopentaose per min under the assay conditions.

Ligand Binding Studies

Fluorescence Measurements

Fluorescence measurements of HPA were carried out in 0.02 M sodium phosphate buffer, pH 6.9 (containing 6 mM NaCl). Fluorescence measurements were performed on a Spectra Max M5 using a λ_{ex} at 280 nm [18-20]. The quenching was performed by titrating 350 µl, 0.29 mM HPA with BDMC (0.001-0.053 mM) (3-45 µl aliquots) followed by monitoring the change in fluorescence at 350 nm.

The data was analyzed by linear fits according to Hegde *et al.* [19] as well as by non-linear regression analysis [20] using the equations

$$(F_0\text{-}F) = (F_0\text{-}F_\infty) \cdot [I_0] / K_d + [I_0] \quad (1)$$

where F and F_0 are the measured fluorescence emission intensity of the protein solution in presence and absence of the ligand, F_∞ when protein is saturated with ligand and I_0 the total concentration of the bound and unbound ligand. The decrease in fluorescence (ΔF) in the presence of different concentrations of the ligand is measured, and the dissociation constant (K_d) calculated.

The calculation of the Gibbs free energy (ΔG^0) was achieved by application of the following equation

$$\Delta G^0 = -RT \ln K_a \quad (2)$$

where R is the gas constant, T the temperature in Kelvin and K_a the association constant.

The enthalpy change (ΔH) and entropy change (ΔS) were calculated by van't Hoff analysis from the temperature dependence of K_a [30] by using the equation

$$\ln K_a = - \Delta H/RT + \Delta S/R \quad (3)$$

The entropy change was then obtained from the equation

$$\Delta G^0 = \Delta H\text{-}T\Delta S \quad (4)$$

Circular Dichroism Spectral Analysis

Circular dichroism (CD) spectra, in the near-uv (250–320 nm) and far–uv (195 to 250 nm) regions were recorded with a Jasco J-815 spectrometer at 100 nm min^{-1}, with a 1-s response time and a 1-nm bandwidth. The quartz cuvette (0.1-cm) contained 50-100 µg of HPA in 0.02M sodium phosphate buffer (pH 6.9). For ligand binding analysis, BDMC at its K_i' was pre-incubated along with HPA for 15 min and CD spectral scans were taken. Appropriate controls of buffer blanks, BDMC in buffer were also performed and the scans corrected.

Docking Simulations

For docking simulations, using AutoDock Vina [21], surface pocket identification of HPA (PDB ID: 1HNY) [22] was carried out on servers CASTp, Pocket-Finder and Q-SiteFinder [23, 24]. Docking protocol and parameters were standardized by performing docking simulation of acarbose pseudopentasaccharide, using Gaussian-09 [25], with HPA, for which a cocrystal structure is available (PDB ID: 1B2Y) [26]. The uncomplexed structure of HPA (1HNY) was first processed to set protonation states of amino acids with polar side chains to neutral pH. Grid box of 80 x 70 x70 points was used with three grid spacings: 0.375, 0.5, and 1.0 A°. The grid box center was set at x = 6.448, y = 46.002, and z = 35.697 A° and gasteiger charges assigned to protein and BDMC. Exhaustiveness level was set on 8 and a computer with four processors was utilized for the computations. A total of 270 docked poses of acarbose pseudopentasaccharide were generated and compared with crystal structure of the complex (1B2Y).

Docking simulations of BDMC with HPA were carried out using the standardized docking parameters obtained. (106 x126 x 126 points), spacing of 0.5 A° and grid box center set at x = 8.499, y = 61.167, and z = 13.444. Based on the outputs of blind docking, refined docking simulation was done with grid parameters that scored high in blind docking. Grid box of 80 x 70 x 70 points was used with a spacing of 0.5 A° and the grid box center set at x = 6.448, y = 46.002, and z = 35.697. The interactions of BDMC-HPA were analyzed and visualized using Insight II software (ver 2000).

Statistical Analysis

Analyses were repeated at least three times and evaluated by their means and standard deviations. The best-fit values were achieved by applying either linear fit or non-linear least square regression using the software, Microcal Origin 6.0 (Micarocal Software Inc., Northampton, USA). Analyses of variance were carried out followed by F-test using the SPSS statistical package (SPSS 11.5).

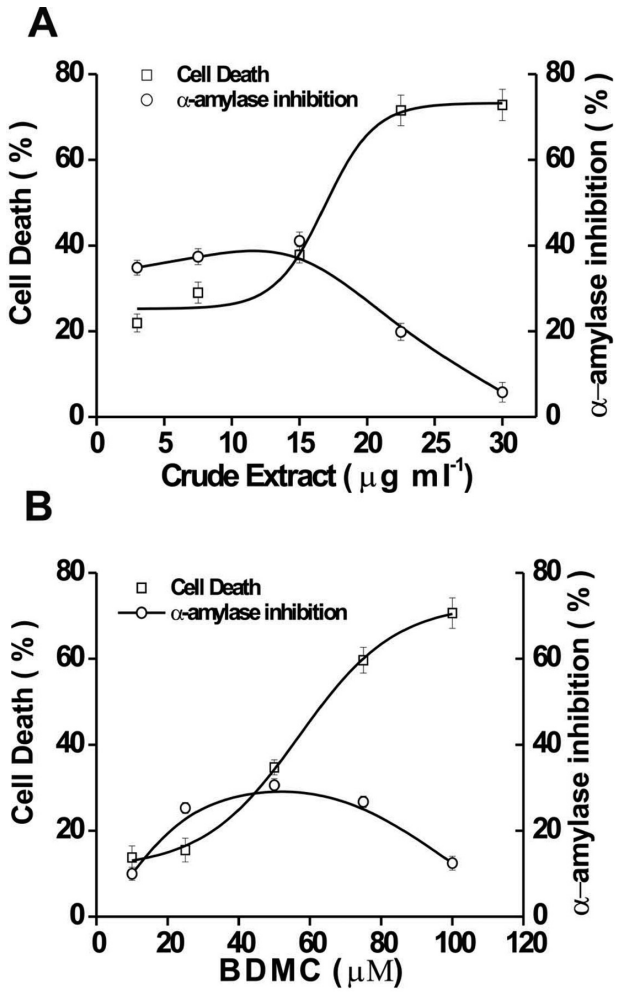

Fig. (1). Cytotoxicity and panceratic α-amylase inhibition in AR42J cell line. A) Effect of crude extract on cell viability and pancreatic α-amylase activity of dexamethasone induced AR42J cell line. **B**) Effect of BDMC on cell viability and pancreatic α-amylase activity of dexamethasone induced AR42J cell line. Error bars represent ±SE of the mean of triplicates and p values < 0.05

RESULTS

Cytotoxicity and Bioactivity

The effect of serum soluble crude and BDMC, on 24 h dexamethaxone induced AR42J cells was determined by MTT assay and the secretory pancreatic α-amylase inhibition is shown in Figs. **1** (**A** & **B**). The resulting growth curve shows that both crude and the purified inhibitor, BDMC have a sigmoidal dose-dependent effect on the rate of cell proliferation. By the MTT technique, crude extract and BDMC exhibit an LD_{50} value of 16.25 µg ml^{-1} and 63.53 µM, respectively. There was no morphological change observed in crude and BDMC treated dexamethasone induced AR42J cell line as compared to the control (Fig. **2**). The maximal secretory pancreatic α-amylase inhibition of 41 and 30 % is observed at 15 µgml^{-1} and 30 µM for crude extract and BDMC, respectively. At these concentrations of both crude and BDMC, varying starch loads exhibited a maximum inhibition of 55 % and 37 % at 0.5 % (w/v) starch respectively.

Inhibition Kinetics of HPA by BDMC

The effect of BDMC on the kinetics of HPA catalyzed hydrolysis of maltopentaose was studied at differing inhibitor concentrations. The double reciprocal LB plots revealed that the mode of BDMC inhibition is uncompetitive for maltopentaose (Fig. **3A**) with decrease in both the apparent K_m and V_{max}. Since the mode of inhibition obtained was uncompetitive, the Bowden plot was subsequently drawn and a K_i' of 0.01mM was obtained for BDMC using maltopentaose as substrate (Fig. **3B**).

Incubation of HPA with BDMC resulted in a time-dependent inactivation (Fig. **3C**) with inactivation following pseudo-first order kinetic behavior using starch as substrate. A reciprocal plot of the pseudo-first order rate constants (k_{obs}) versus inhibitor concentration (Fig. **3D**) yielded a value of k_i/K_i' of 1.72 min^{-1} mM^{-1} for HPA.

BINDING OF BDMC

Fluorescence Studies

Fig. (**4**) shows the dependence of decrease in fluorescence intensity at 350 nm on the binding of BDMC to HPA while ΔF is the decrease in fluorescence intensity relative to the fluorescence intensity of the free enzyme on ligand binding. HPA (16.6 µg) bound to maltose exhibited a fluorescence intensity of 210 a.u. with a λ_{max} emission of 350 nm. Titration of this enzyme-maltose complex with BDMC (0.001-0.053 mM) resulted in quenching of the intrinsic fluorescence to 68 a.u. with maximal quenching of 68 % and

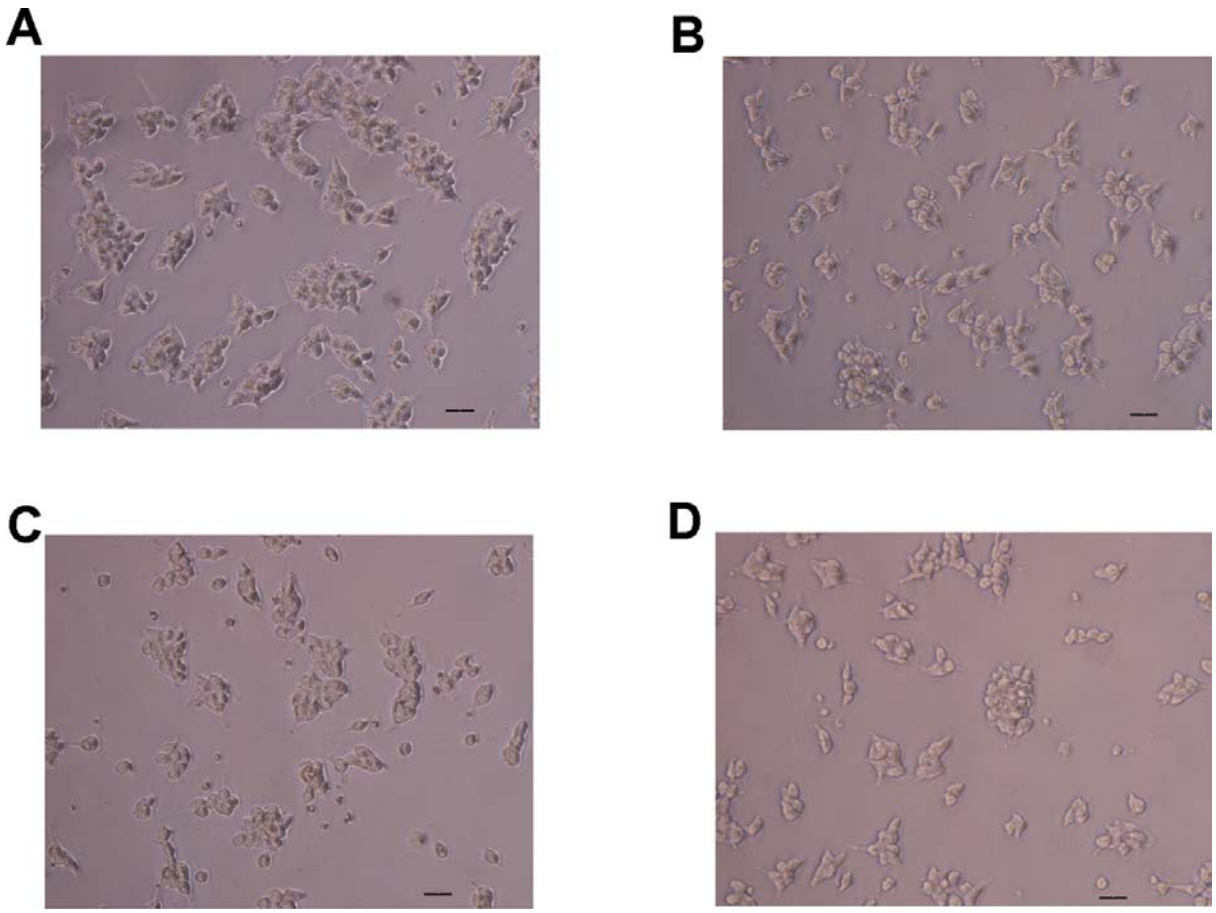

Fig. (2). Effect on Morphology of AR42J cell line. Inverted phase contrast image under magnification of 200 X of AR42J cell lines treated under following conditions. **A**) Control **B**) 10nM Dexamethasone induced **C**) Crude extract at 15µgml^{-1} **D**) BDMC at 30 µMml^{-1} The scale

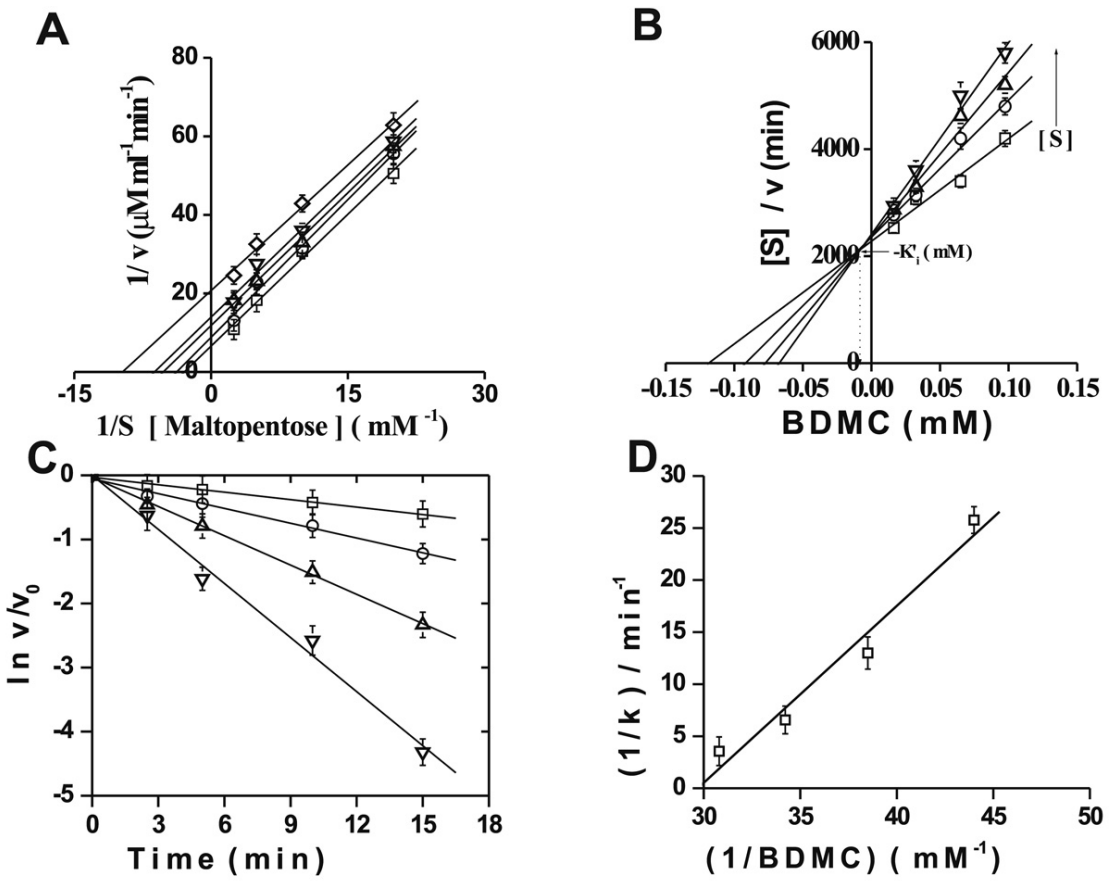

Fig. (3). Kinetic Analysis of HPA Inhibition by BDMC. A) LB plot for HPA inhibition at varying BDMC concentrations □, 0 mM; ○, 0.016 mM; Δ, 0.032 mM; ▽, 0.064 mM; ◊; 0.097 mM with maltopentaose as substrate. **B**) Bowden plot with varying concentrations of maltopentaose □, 0.05 mM; ○, 0.1 mM; Δ, 0.2 mM; ▽, 0.4 mM. **C**) Semi-logarithmic plot of activity *versus* time □, 0.022 mM; ○, 0.025 mM; Δ 0.029 mM; ▽, 0.032 mM). **D**) Replot of first-order rate constants from Fig. (**3C**). Error bars represent ±SE of mean of triplicates and $p<0.05$ were considered significant.

no shift being observed in λ_{max} emission (Fig. **4A**). The unbound HPA (16.6 μg) with an activity of 0.25 U ml^{-1} exhibited a fluorescence intensity of 225 a.u. with a λ_{max} emission also at 350 nm. Titration resulted in quenching of the intrinsic fluorescence to 67 a.u. with maximal quenching of 70 % and no change in λ_{max} emission (Fig. **4B**). No emission was noted in the same region for BDMC alone under any of the abovementioned conditions. The fluorescence spectra and quenching pattern of BDMC binding to both unbound HPA and maltose bound HPA were similar. The calculation of binding parameters such as the dissociation and association constants (K_d and K_a) was performed by the linear as well as non-linear regression analysis [18, 19]. Fig. (**4A**), B show the non-linear fits for titration at 25ºC of BDMC with HPA-maltose complex, unbound HPA and with R^2 values of 0.997, 0.997 respectively. These high R^2 values suggest the one-site binding model. The K_d values ascertained from the fits exhibited values of 20.05 x 10^6 and 11.77 x 10^6, respectively for the maltose complexed, and unbound HPA at 25ºC.

Circular Dichroism Studies

The effect of binding on secondary and tertiary structure ellipticity plotted. The far uv-CD spectra (195-250 nm) for HPA in this study were in accordance with the reported spectra for mammalian amylases [27, 28]. However, no significant change in the secondary structural elements was observed on binding of BDMC to HPA (Fig. **5A**). The CD spectrum of a protein in the near-UV spectral region (250–350 nm) is sensitive to perturbations of tertiary structure. At these wavelengths, the chromophores involved are the aromatic amino acids which can reflect changes in tertiary structure on binding. Fig. (**5B**) shows the effect of addition of BDMC on the CD spectra of HPA in the region 250–320 nm. The major changes in spectra of HPA can be attributed to the change in environment of phenylalanine at 260 nm and tryptophan at 290-310 nm, on binding of BDMC. No significant structure was noted either in the far-or near-uv region for BDMC alone under the same conditions. In an earlier study, the binding of Cys3glc to Porcine pancreatic α-amylase (PPA) resulted in an alteration in the environment of phenylalanine residues [18].

Thermodynamic Parameters

Since K_a varies with temperature, the binding parameters of BDMC to HPA were carried out at different temperatures

DOCKET ALARM

Explore Litigation Insights

Docket Alarm provides insights to develop a more informed litigation strategy and the peace of mind of knowing you're on top of things.

Real-Time Litigation Alerts

Keep your litigation team up-to-date with **real-time alerts** and advanced team management tools built for the enterprise, all while greatly reducing PACER spend.

Our comprehensive service means we can handle Federal, State, and Administrative courts across the country.

Advanced Docket Research

With over 230 million records, Docket Alarm's cloud-native docket research platform finds what other services can't. Coverage includes Federal, State, plus PTAB, TTAB, ITC and NLRB decisions, all in one place.

Identify arguments that have been successful in the past with full text, pinpoint searching. Link to case law cited within any court document via Fastcase.

Analytics At Your Fingertips

Learn what happened the last time a particular judge, opposing counsel or company faced cases similar to yours.

Advanced out-of-the-box PTAB and TTAB analytics are always at your fingertips.

API

Docket Alarm offers a powerful API (application programming interface) to developers that want to integrate case filings into their apps.

LAW FIRMS
Build custom dashboards for your attorneys and clients with live data direct from the court.

Automate many repetitive legal tasks like conflict checks, document management, and marketing.

FINANCIAL INSTITUTIONS
Litigation and bankruptcy checks for companies and debtors.

E-DISCOVERY AND LEGAL VENDORS
Sync your system to PACER to automate legal marketing.